Carbohydrate Polymer Technologies and Applications 2 (2021) 100084

Contents lists available at ScienceDirect

Carbohydrate Polymer Technologies and Applications

journal homepage: www.elsevier.com/locate/carpta

Fabrication of radiation cross-linked diclofenac sodium loaded carboxymethyl sago pulp/chitosan hydrogel for enteric and sustained drug delivery

Li Shan Tan[a], Hui Li Tan[a], Karthik Deekonda[a], Yeon Yin Wong[a], Saravanan Muniyandy[c], Kamaruddin Hashim[d], Janarthanan Pushpamalar[a,b,*]

[a] School of Science, Monash University Malaysia, Jalan Lagoon Selatan, 47500 Bandar Sunway, Subang Jaya, Selangor Darul Ehsan, Malaysia
[b] Monash-Industry Palm Oil Education and Research Platform (MIPO), Monash University Malaysia, Jalan Lagoon Selatan, Bandar Sunway, 47500 Selangor Darul Ehsan, Malaysia
[c] Department of Pharmacy, Fatima College of Health Sciences, P.O. Box 24162 Al Maqam, Al Ain, United Arab Emirates
[d] Radiation Modification of Polymer Group, Radiation Processing Technology Division, Malaysian Nuclear Agency, 43000 Bangi, Selangor Darul Ehsan, Malaysia

ARTICLE INFO

Keywords:
Carboxymethyl sago pulp/chitosan
Sustained drug delivery
Radiation cross-linking

ABSTRACT

Carboxymethyl sago pulp (CMSP) with a degree of substitution 0.8 was synthesised from sago waste and cross-linked with chitosan to form a hydrogel by electron beam (EB) irradiation. Diclofenac sodium was loaded into 40% CMSP/3% chitosan solution mixture and irradiated at 25 kGy. The hydrogel exhibited pH and temperature-sensitive swelling behaviour. Fourier-transform infrared spectroscopy, field emission scanning electron microscope, X-ray diffraction, differential scanning calorimetry, and thermogravimetric analysis were performed to characterise its properties. Drug entrapment efficiency of diclofenac sodium-loaded hydrogel was 65.4 ± 0.2%. The release of diclofenac sodium from CMSP/chitosan hydrogel disc was low in an acidic environment (pH 1.2) and there was slow and sustained release in colonic pH (pH 6.8) over 32 h in a first-order manner. Based on the results of the disk diffusion test, the hydrogel exhibited antimicrobial activity against the tested microorganisms. Among tested formulations, 40% CMSP/3% chitosan hydrogel was shown to be the potential drug carrier for sustained drug delivery.

1. Introduction

Colorectal cancer (CRC) has been known as the third leading cause of cancer-related mortality in North America, causing about 49,190 deaths in 2016 (O'Neill, Nguemo, Tynan, Burchell, & Antoniou, 2017). Among various administration routes, rectal administration offers the shortest route to deliver the drug to the colon, but it creates unpleasant feeling and inconvenience to the patients. Therefore, oral administration of the drug becomes the most widely accepted route. However, it has limitations such as degradation or release of drug in the stomach and small intestine rather than the colon, causing low bioavailability (Rajpurohit, Sharma, Sharma, & Bhandari, 2010). As the number of CRC cases has increased drastically, the development of a controlled drug delivery system to the colon is of utmost importance to achieve a better therapeutic effect.

Recently, hydrogels from natural polymers have drawn much interest from scientists from biomedical and pharmaceutical areas due to their biodegradability, biocompatibility, biosafety, high hydrophilicity, and high availability Chang & Zhang (2011). One of the examples of polymer used for these applications is carboxymethyl cellulose (CMC). CMC is an anionic polysaccharide derived from cellulose, with the substitution of carboxymethyl groups to some hydroxyl groups of cellulose by glycoside bonds Chen & Cooper (2002). As a water-soluble polysaccharide, it dissolved in water and became negatively charged due to the dissociation of carboxyl groups (Prado da Silva et al., 2014). CMC can be derived from cellulose of various kinds of sustainable resources such as bamboo, cotton, flax, hemp, jute, sisal, banana, and straws (rice and wheat) (Reddy, Uma Maheswari, Muzenda, Shukla, & Rajulu, 2016). Our previous work reported on CMC preparation from biomass waste from sago palm (Metroxylon sagu), and it is specifically known as carboxymethyl sago pulp (CMSP) (V. Pushpamalar, Langford, Ahmad, & Lim, 2006). In our previous studies, CMSP with the degree of substitution of 0.4 has been used to prepare hydrogel beads and discs for drug delivery applications (Lam, Muniyandy, Kamaruddin, Mansor, & Janarthanan, 2015; Thenapakiam, Kumar, Pushpamalar, & Saravanan, 2013). Besides, CMSP with the degree of substitution of 0.8 have been cross-linked with other polysaccharides such as carboxymethyl sago starch and pectin using EB irradiation to form hydrogels (Tan et al., 2016a and Tan, Wong, Muniyandy, Hashim, & Pushpamalar, 2016b). In a recent study, poly(lactic acid)/CMC/curcumin film was prepared, for

* Corresponding author.
E-mail address: pushpa.janarthanan@monash.edu (J. Pushpamalar).

https://doi.org/10.1016/j.carpta.2021.100084
Received 15 February 2021; Received in revised form 26 April 2021; Accepted 1 May 2021
Available online 7 May 2021

improvement of curcumin release in the intestinal alkaline environment (Sampath U. Gunathilake, Ching, Chuah, Rahman, & Nai-Shang, 2020). Electrically controlled release of drug from CMC hydrogel has also been reported (Sangsuriyonk, Paradee, & Sirivat, 2020).

Chitosan is a long-chain polysaccharide made up of N-acetyl-D-glucosamine and D-glucosamine units linked by β-(1-4)-glycosidic bonds (Alves & Mano, 2008). It is a polycationic polymer with two hydroxyls (-OH) groups and one amino (-NH_2) group in repeating glycosidic residue. The presence of active primary amino groups in chitosan structure can provide an active site for many side-groups and thus alter its biological and physical properties. Due to its interesting properties such as bioadhesion, biodegradability, and biocompatibility, chitosan has been used to develop hydrogels for drug delivery purposes (Martinez-Ruvalcaba, Sánchez-Díaz, Becerra, Cruz-Barba, & González-Álvarez, 2009; Pourjavadi, Jahromi, Seidi, & Salimi, 2010). Stimuli-responsive hydrogel such as thermal sensitive poloxamer/chitosan hydrogel has been developed for mucosal drug delivery. UV and pH-responsive chitosan hydrogel was synthesised using a photocleavable crosslinker (Nisar, Pandit, Wang, & Rattan, 2020).

In a study, blend hydrogel of CMC and chitosan has been prepared using EB irradiation. The reported biodegradability of this hydrogel opens up its potential applications in the biomedical area Zhao & Mitomo (2008). To further characterise the prepared CMSP with the degree of substitution of 0.8 and explore the potential application of the blend hydrogel of CMC and chitosan, this study aimed to prepare EB-crosslinked hydrogel made of CMSP and chitosan for drug delivery application. The advantages of using EB irradiation for cross-linking are that no additives are required and reduces production cost Zhao & Mitomo (2008). In this study, CMSP/chitosan hydrogel discs are incorporated with diclofenac sodium, a non-steroidal anti-inflammatory drug with analgesic and antipyretic properties Khan (2012). It was chosen as the model drug in this study because it also has an antiproliferative effect against cancer cell growth, and it can be used for the treatment of colorectal cancer (Nargave, Singh, & Kondalkar, 2016). In this study, gel fraction, swelling property, drug release behaviour, and antimicrobial activity of CMSP/chitosan hydrogel were determined. Also, the hydrogel discs were characterised using Fourier-transform infrared spectroscopy, field emission scanning electron microscope, X-ray diffraction, differential scanning calorimetry, and thermogravimetric analysis.

2. Materials and methods

2.1. Materials

Sago waste was obtained from Ng Kia Heng, Kilang Sagu Industrial Sdn. Bhd, Johor, Malaysia, Diclofenac sodium was purchased from Ningbo Hi-tech Biochemicals Co. Ltd., China. Methanol, isopropanol and ethanol (denatured 95%), sodium hydroxide pellets, glacial acetic acid, were obtained from Friedemann Schmidt, Malaysia. Sodium chlorite (80% technical grade) and chitosan (75–85% deacetylated, low molecular weight) were obtained from Sigma–Aldrich. Sodium monochloroacetate was obtained from Fluka.

2.2. Isolation of sago pulp

Sago waste was pre-dried in the oven for 3 h, ground using a blender and sieved through 0.5 mm^2 test sieve. The ground sago waste was pre-dried at 60 °C for 1 h. Twenty grams of sago waste was transferred into a 1 L conical flask and suspended in 640 mL of hot distilled water followed by the addition of 4 mL of glacial acetic acid and 6 g of sodium chlorite. The conical flask was placed in a water bath maintained at 70 °C for 3 h. The mixture was filtered using a cheesecloth funnel and washed with cold distilled water until the filtrate reaches pH 7. The residue was then dried in an oven at 70 °C until constant weight (V. Pushpamalar et al., 2006).

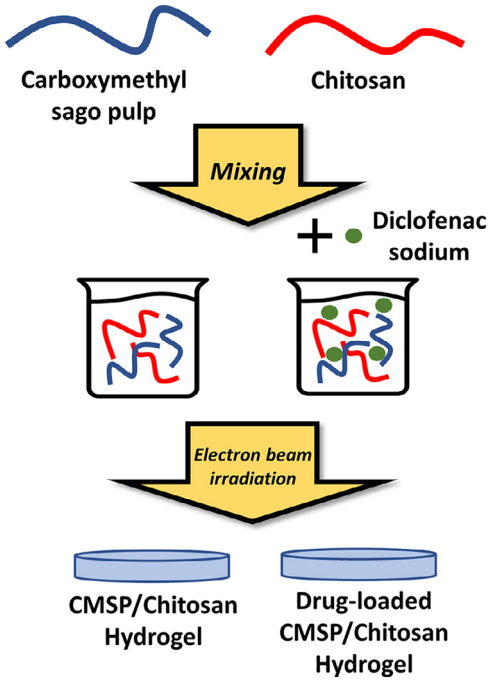

Fig. 1. Schematic diagram of CMSP/chitosan hydrogel preparation.

2.3. Preparation of carboxymethyl sago pulp with degree of substitution of 0.8

Five grams of sago pulp was added into 250 mL Scott bottle filled with 100 mL of isopropanol. Sodium hydroxide (10 mL of 25% w/v) was added dropwise. The mixture was stirred for an hour at 160 rpm, and 6 g of sodium mono chloroacetate was added to the mixture. The mixture was shaken in a water bath at 190 rpm and 45 °C for 3 h. The mixture was then filtered using the Buchner funnel, and the residue was suspended overnight in 300 mL methanol. The suspended solution was neutralised using glacial acetic acid and then filtered using the Buchner funnel. The residue was washed with 300 mL ethanol to remove unwanted products and dried in an oven at 70 °C until constant weight (V. Pushpamalar et al., 2006).

2.4. Preparation of diclofenac sodium loaded CMSP/chitosan hydrogel discs

A series of concentrations of CMSP with degree of substitution 0.8 solutions (10%, 20%, 30% and 40% (w/v)) were prepared. The chitosan (2% and 3%) were dissolved separately in 1% acetic acid overnight at 1000 rpm. Twenty-five millilitres of 10% of CMSP was mixed with 5 mL of 2% chitosan using a stirrer at 1000 rpm for 2 h. The CMSP/chitosan mixture appeared as a turbid viscous solution, and 30 mL of the mixture was poured separately into the lids of the petri dish. The EB irradiation doses were 20, 25, 30, 40 and 50 kGys using an EB accelerator (EPS-3000, 2 MeV energy, 10 mA current and 20 kW power), at room temperature (25 °C), in air using a dose rate of 5 kGy/pass. The preparation of hydrogel is illustrated in Fig. 1.

2.5. Determination of gel fraction

All irradiated samples were weighed (W_0) and poured into individual tea bags, and suspended overnight in distilled water to obtain the insoluble hydrogels. The insoluble hydrogel was transferred into individual plastic bags and dried at 70°C until constant weight (W_1). The percentages of soluble fraction and gel fraction were calculated as shown in Eq. 1 and 2 (Vengidesh Pushpamalar, Langford, Ahmad, Hashim, &

Lim, 2013):

$$\text{Sol fraction (\%)} = \frac{W0 - W1}{W0} \times 100 \quad (1)$$

$$\text{Gel fraction (\%)} = 100 - \text{Sol fraction} \quad (2)$$

2.6. Preparation of diclofenac sodium loaded CMSP/chitosan hydrogel discs

The 30% (w/w) of diclofenac sodium based on CMSP and chitosan weight was dissolved in 25 mL of distilled water and covered with aluminium foil to protect the solution from light. A 25 mL of 40% (w/v) of CMSP was added to the solution and stirred for an hour. Five millilitres of 3% chitosan were added and mixed using a stirrer at 1000 rpm for 2 h. Thirty millilitres of CMSP/chitosan mixture were poured separately into the lids of the petri dish and irradiated at 25 kGy using EB accelerator. The samples were dried in an oven at 70 °C until constant weight. Circular discs were cut using 6 mm single hole puncher. The unloaded discs were prepared using the same method without the addition of drug.

2.7. Determination of drug loading and drug entrapment efficiency (DEE)

Diclofenac sodium-loaded discs (250 mg) were placed in Schott bottles containing 100 mL of 1 N NaOH and stirred at 200 rpm and 40 °C for 24 h to extract the drug. The samples were collected, filtered, diluted, and absorbance was measured at 276 nm using a Shimadzu UV-1800 UV–vis spectrophotometer. Drug loading and DEE were calculated using Eq. 3 and 4 (Thenapakiam et al., 2013):

$$\text{Drug Loading in \%} = \frac{\text{Drug content of hydrogel disc}}{\text{Weight of hydrogel disc}} \text{ x } 100\% \quad (3)$$

$$\text{DEE} = \frac{\text{Drug content of hydrogel disc}}{\text{Theoretical drug content of hydrogel disc}} \text{ x } 100\% \quad (4)$$

2.8. Hydrogel discs analysis

Diameter, thickness and weight of diclofenac sodium-loaded and unloaded CMSP/chitosan discs were measured using a dial calliper (Series 505, Mitutoyo, JAPAN) and an electronic balance (Sartorius, Germany).

2.9. Field emission scanning electron microscopy (FESEM) analysis

Chitosan, CMSP, and diclofenac sodium-loaded and unloaded CMSP/chitosan discs were initially coated with a thin layer of platinum using a Q150R S rotary-pumped sputter coating system (Quorum Technologies, UK) before being observed at different magnifications using FESEM (SU8010, Hitachi, Japan)

2.10. Fourier transforms infrared (FTIR) spectrometry

CMSP, chitosan, unloaded and diclofenac sodium-loaded CMSP/chitosan discs were grounded into powders and the spectra between 600 and 4000 cm^{-1} were obtained using an FTIR spectrophotometer using attenuated total reflection accessory (Varian, USA).

2.11. X-ray diffraction (XRD)

Diffractograms of sample powders were obtained over a 2θ range from 5–70°. A Bruker D8 DISCOVER X-ray diffraction apparatus was used. The analysis was performed with a cobalt target X-ray tube operating at 30 kV and 330 μA.

2.12. Differential scanning calorimetry (DSC)

DSC was carried out with the range of temperature 30 to 400 °C on DSC 4000 (Perkin Elmer, USA). 5 mg of sample was sealed into aluminium pans. The heating rate was 15 °C min^{-1} while 20 °C min^{-1} for nitrogen flow rate.

2.13. Thermogravimetric analysis (TGA)

TGA was performed on TGA/DSC 2 (METTLER TOLEDO, USA). Ten milligrams of samples were analysed at a range of 60 to 600 °C with a heating rate of 10 °C min^{-1} and nitrogen flow rate of 50 mL min^{-1}.

2.14. Swelling behaviour

The swelling behaviour of the unloaded CMSP/chitosan disc was studied in distilled water and various pH media. Dry hydrogel discs (0.5 g) were immersed in excess distilled water and buffer solutions at pH 1.2, 5.5 and 7.4, respectively at room temperature (25 °C). The swollen discs were removed from the solution and weighed. The excess surface liquid of the hydrogel disc was blotted using filter paper. The swelling percentage was calculated using Eq. 5:

$$\%S = \frac{Mt - M0}{M0} \text{ x } 100 \quad (5)$$

where M0 is a mass of dry hydrogel disc at a 0th time, and Mt is a mass of swollen hydrogel disc at a specific time, up to 24 h (Tan et al., 2016a).

2.15. Drug release kinetics

The *in vitro* release studies were carried out in a USP dissolution tester (TDT-08L) by paddle method at a rotation speed of 50 rpm in 900 mL medium at 37.0 ± 0.5 °C. The continuous changing pH dissolution method was used to simulate the gastrointestinal tract environment. Firstly, drug-loaded discs were added to 675 mL of 0.1 N HCl (pH 1.2) for 2 h. After 2 h, 225 mL of tribasic sodium phosphate solution was added to the chambers through dissolution vessels, and the pH was adjusted to 6.8 using 2 M NaOH or 2 M HCl if necessary. The drug-loaded discs ($n = 11$) were placed in individual chambers, and 5 mL of aliquots were withdrawn at regular intervals and replaced with the same amount of release medium. The aliquots were collected using a 5 mL syringe and filtered. The amount of drug present in the aliquots was determined and analysed by UV-1800 UV-Vis spectrophotometer at 276 nm (Tan et al., 2016a).

The drug release kinetics were analysed. The zero-order release kinetics describes the constant release of drug from drug delivery device with hydrophobic drug. A graph of Q_t versus t was plotted to show the zero-order kinetics model. The equation was shown below:

$$Qt = Q0 + K0t \quad (6)$$

However, a graph of log (Q_0-Q_t) versus t was plotted as a first-order kinetic model where it describes that the release of the drug is proportional to the amount of drug remaining in the interior of the drug delivery device with a hydrophilic drug with the equation shown below:

$$\log Qt = \log Qo - Kt / 2.303 \quad (7)$$

where Q_t is the quantity of drugs released at time t, and the initial quantity of the drug entrapped in the drug-loaded disc is represented by Q_o (Gibaldi & Feldman, 1967; Mulye & Turco, 1995).

2.16. Antimicrobial activity of CMSP/chitosan hydrogel discs

The antimicrobial properties of the hydrogels were investigated utilising agar disk diffusion method. Four CMSP/chitosan discs consisting of (a) CMSP: chitosan (20:2 w/w%, unloaded) (b) CMSP: chitosan (30:2 w/w%, unloaded) (c) CMSP: chitosan (40:2 w/w%, loaded with 16.75%

of diclofenac sodium) and (d) CMSP: chitosan (40:3 w/w%, loaded with 19.61% of diclofenac sodium) were used. Six bacterial strains were chosen: two gram+ and four gram- clinical pathogen which included methicillin-resistant *Staphylococcus aureus* (gram+, ATCC 700699), *Enterococcus faecalis* (gram+, ATCC 2921), *Klebsiella pneumoniae* (gram-, ATCC 10031), *Proteus mirabilis* (gram-, ATCC 12453), *E. coli* (gram-, ATCC 25922), *Pseudomonas aeruginosa* (gram-, ATCC 10145). The nutrient broth required for the overnight bacterial cultures was prepared by dissolving 3.7 g of Merck nutrient broth (Kenilworth, New Jersey, United States) in 100 ml of 18.1 MΩ distilled water. The nutrient broth was sterilised by autoclaving at 121 °C for 15 min and cooled down to 37 °C. Approximately 5 ml of nutrient broth was poured into six 15 ml centrifuge tube along with 1 ml inoculum of the glycerol stock of bacterial strains and incubated at 37 °C for 18 h at 200 rpm. The agar plates were prepared by specifically dissolving 13.5 g of Merck nutrient agar (Kenilworth, New Jersey, United States) in 500 ml of 18.1 MΩ distilled water. The nutrient agar was sterilised by autoclaving at 121 °C for 15 min, cooled down to 37 °C, and 20 ml was poured into each Petri dish and allowed to form an agar gel. The Petri dishes were inoculated with each bacterial strain by spread plate method. 100 µl of the overnight culture was pipetted onto each place and spread evenly using a sterile L-rod, followed by placing the CMSP/Chitosan discs onto the Petri dishes. The Petri dishes were labelled accordingly and incubated at 37 °C for 24 h to obtain the inhibition zone (Wen et al., 2016).

2.17. Statistical analysis

Each experiment was performed at least in triplicates. All data were shown as means ± standard deviation. IBM SPSS Statistics software version 20 was used to analyse results with a *p*-value of 0.05 using one-way-ANOVA.

3. Results and discussion

3.1. Preparation of hydrogel discs

CMSP/chitosan hydrogel discs formed from 40%/2% and 40%/3% (CMSP/chitosan) polymer solutions were shown to be intact, firm, and thicker, whereas 10%/2% and 10%/3% (CMSP/chitosan) hydrogels appeared to be fragile and thinner. The difference in hydrogel formation indicated that higher concentration of both polymers were required to form a more robust hydrogel.

3.2. EB irradiation on hydrogel

During EB irradiation, radical cross-linking or scission process could occur. Radical cross-linking occurred when free radicals are recombined together. On the other hand, scission process occurred when there was a failure of radical-radical reactions, thus terminated by reactions with oxygen and/or hydrogen abstraction (Fei, Wach, Mitomo, Yoshii, & Kume, 2000). Recombination of radicals formed at the side chain causes cross-linking, whereas the recombination of radicals formed at the glycoside bond causes degradation (Yoshii et al., 2003). CMC polymers were found to cross-link and form a hydrogel when there was a high concentration of polymers. Chitosan provides an additional cross-link site with CMC through ionic interaction or hydrogen bond. Besides, it promotes cross-linking through stimulation of radical formation and sustainment for the life of radicals Zhao & Mitomo (2008).

The cross-linking degree of hydrogels from irradiation reaction was characterised using gel fraction analysis. Based on Fig. 2 (a) and (b), gel fraction of 10%/2%, 20%/2%, 30%/2%, 40%/2%, 10%/3%, 20%/3%, 30%/3% and 40%/3% (CMSP/chitosan) hydrogels increased as the irradiation dose increased. However, when the gel fraction reached a maximum point, it started to decrease despite the increase of irradiation dose. The maximum percentage of gel fraction for all hydrogels achieved at around 25–30 kGy. The presence of water in polymer solution was essential for maximum cross-linking because water increases the mobility of rigid molecules of CMSP by allowing macro-radicals to recombine with each other. Besides, hydrogen atoms and hydroxyl radicals can induce more macro-radicals by hydrogen abstraction from CMSP molecules (Vengidesh Pushpamalar et al., 2013; Yoshii et al., 2003). There was intermolecular and intramolecular recombination of macro-radicals. Intermolecular recombination leads to the linkage between two radicals on separate chains, whereas intramolecular recombination leads to the formation of a C-C bond between segments of the chain itself (Ulański, Janik, & Rosiak, 1998). Therefore, the reduction in the percentage of gel fraction beyond 25 kGy might be due to the predominant of chain scission process and oxidative degradation as compared to cross-linking.

3.3. Effect of CMSP and chitosan concentration on gel fraction of hydrogel

As shown in Fig. 2(c) and (d), hydrogels with 30–40% CMSP with 2–3% chitosan showed higher gel fraction when there was an increase in CMSP content. The increase in gel fraction could be due to a higher probability for each CMSP macromolecular radical to form a hydrogel. Thus, cross-linking predominates degradation (Vengidesh Pushpamalar et al., 2013). Two radicals of CMSP chains have recombined to form intermolecular cross-linking and resulted in the formation of an insoluble gel. On the other hand, CMSP/chitosan undergo degradation in the diluted polymer solution. As the concentration decreases, the density of macro-radicals decreases. Radical-radical reactions cannot be promoted to form cross-links due to the larger distance between macro-radicals. Consequently, the degradation process predominates (Vengidesh Pushpamalar et al., 2013).

Interestingly, it was also found that the percentage of gel fraction be significantly reduced when the concentration of chitosan increased, as shown in Fig. 2(c) and (d). This might be due to the higher concentration of chitosan that hindered the recombination of radicals. Hence, the occurrence of the cross-linking process has been reduced (Tahtat et al., 2011).

3.4. Swelling kinetics

The 20%/2%, 20%/3%, 30%/2%, 30%/3%, 40%/2% and 40%/3% CMSP/chitosan hydrogels were chosen for swelling studies as they were stable and stayed intact in the swelling media. Other than distilled water, three media in different pH (pH 1.2, 5.5 and 7.4) were used to study the effect of pH on the swelling properties. These pHs represented the pH of common human body components such as stomach pH (pH 1.2), skin (pH 5.5), and body fluids (pH 7.4) (Almáši et al., 2020; Bashir, Teo, Naeem, Ramesh, & Ramesh, 2017; Seong, Yun, & Park, 2018). The finding could be useful in predicting the swelling behaviour of the hydrogels regardless of which type of drugs they are carrying.

The swelling percentage of hydrogel increased as immersion time increased until it reached a plateau. The swelling percentage of 40% CMSP/3% chitosan hydrogel in distilled water was the highest, 722.75% (Fig. 3(a)). This could be due to the presence of a higher proportion of the hydrophilic polymer content per unit weight in this formulation. This caused a higher affinity for water and an increase in water uptake (Thenapakiam et al., 2013).

Based on Fig. 3(b), CMSP/chitosan hydrogel showed low swelling percentage. As the dissociation constant (pKa) value of CMSP was between 3.8 to 4.2, and at pH 1.2, the COO- group will be protonated to COOH (Martinez-Ruvalcaba et al., 2009; Pourjavadi et al., 2010). For chitosan, it has a pKa value of approximately 6.3. There was protonation of amines (NH_2) to form positively charged ions (NH_3^+). The intermolecular hydrogen bonding between the COOH group from CMSP and NH_3^+ group from chitosan caused the formation of the compact structure of hydrogel that restricted significant swelling of hydrogel disc in an acid environment (Lina Zhang, Jin, Liu, & Du, 2001).

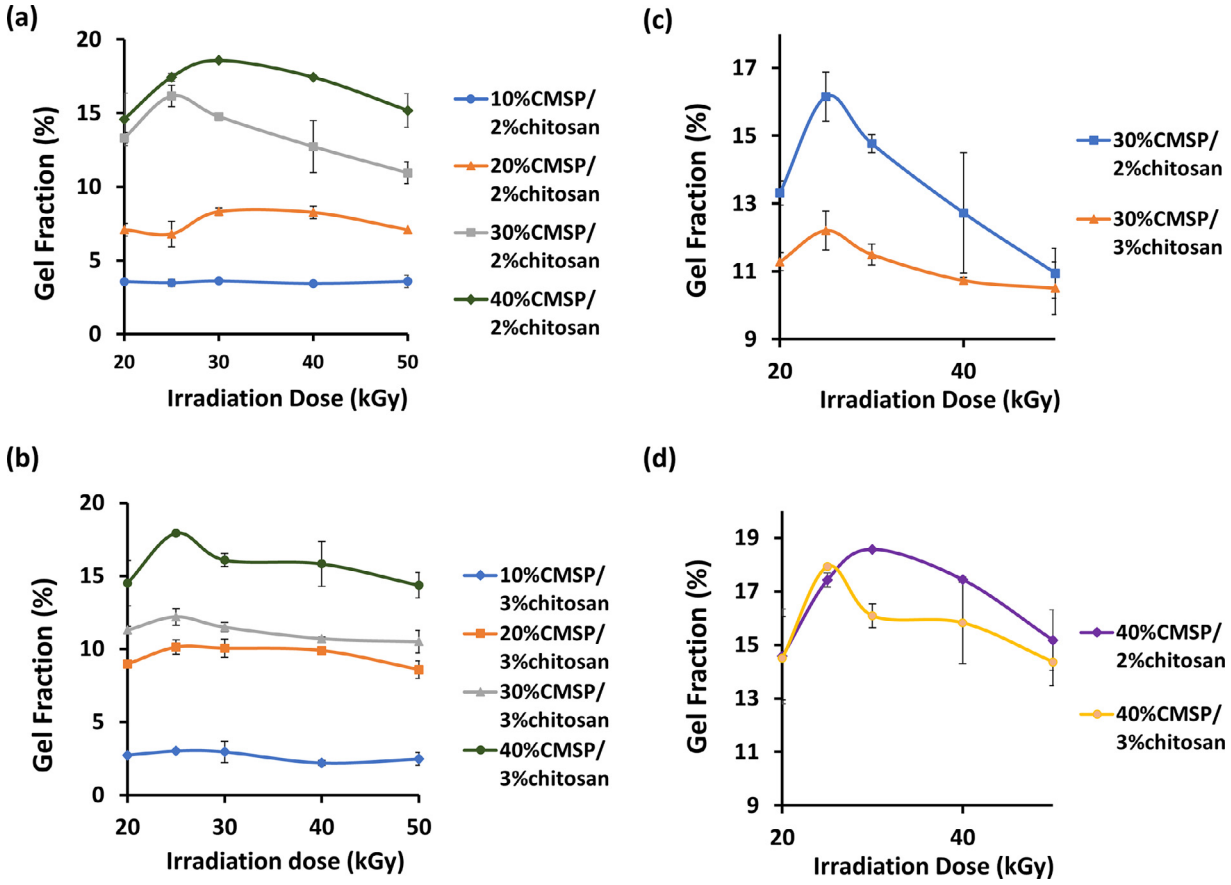

Fig. 2. Graph of gel fraction against EB irradiation dose for (a) 2%, (b) 3% of chitosan with 10%, 20%, 30% and 40% of CMSP, (c) 30% CMSP and (d) 40% CMSP with 2% chitosan and 3% chitosan in hydrogel mixture.

The highest swelling percentage achieved in pH 5.5 buffer was 519.52% by 40% CMSP/2% chitosan hydrogel (Fig. 3(c)). Buffer solution at pH 5.5 was above the pKa value of CMSP, ionisation of the carboxyl group in CMSP occurred. However, pH 5.5 was lower than the pKa value of chitosan, where there was protonation of amines to form positively charged ions. Therefore, there was the formation of electrostatic interaction between free carboxylic groups of CMSP and free amino groups of chitosan. The swelling percentage of all formulation in pH 5.5 was higher than pH 1.2 but lower than pH 7.4. It was concluded that the swelling percentage increases with the increase in pH. This could be explained by the formation of carboxylic anions in the polymer network, which leads to the expansion of the network due to strong electrostatic forces Long & Luyen (1996).

The highest swelling percentage achieved in pH 7.4 buffer was 661.90% by 40% CMSP/3% chitosan hydrogel (Fig. 3 (d)). At pH 7.4, there was ionisation of the carboxyl group in CMSP, whereas deionisation of ammonium into the amino group in chitosan resulted in a decrease in the electrostatic interaction of the amine group of chitosan with the carboxyl group of CMSP. Thus, a less compact structure was formed, allowing water to be trapped inside the hydrogel. Therefore, as more water molecules could diffuse into the hydrogel matrix, it caused the hydrogel to swell Zhao & Mitomo (2008). Based on these results, the pH-sensitive behaviour of the hydrogel has been demonstrated due to the different swelling degree in the buffers at different pH. Besides, the swelling degree might be affected by the ionic strength of the solution. Highest swelling degree of the hydrogel was observed in water due to the higher osmotic pressure difference between the solution and hydrogel as compared to the buffered media that contained salts (Pandey, Mohd Amin, Ahmad, & Abeer, 2013).

The 40% CMSP/3% chitosan hydrogel disc was chosen for further characterisation due to its high swelling at pH 7.4. As seen in Fig. 3(e), the swelling percentage of 40% CMSP/3% chitosan hydrogel increased until a maximum point then decreased. This was different from the swelling behaviour of the similar hydrogel at room temperature (Fig. 3(d)). At room temperature, the high swelling degree was contributed by the interactions between water and polymer chain through hydrogen bonding. At a higher temperature, 37°C, there was a lower swelling degree due to disruption of polymer-water hydrogen bonds and an increase in polymer-polymer interaction. The hydrophobic interactions among hydrophobic segments became strengthened. As a result, there was shrinkage of a hydrogel matrix, due to inter-polymer chain association through hydrophobic interactions Qiu & Park (2001). This explained the eventual decrease in swelling of the hydrogel as time progressed. Based on this result, the swelling behaviour of CMSP/chitosan was demonstrated to be pH and temperature-sensitive. Temperature and pH are crucial environmental factors in physiological, biological, and chemical systems. As there is increasing demand in controlled drug delivery with high precision, the dual-sensitive swelling behaviour of the hydrogel could be beneficial for the controlled release of drug (Fan, Tian, & Liu, 2019).

3.5. *Drug loading and entrapment efficiency*

UV-visible spectrophotometry is a common approach used for the analysis of diclofenac sodium in pharmaceutical formulations (Bucci, Magrì, & Magrì, 1998). Diclofenac sodium (30% w/w) was added during the preparation CMSP/ chitosan hydrogel, and the drug encapsulation efficiency was found to be about 56-65% (Table 1). The drug

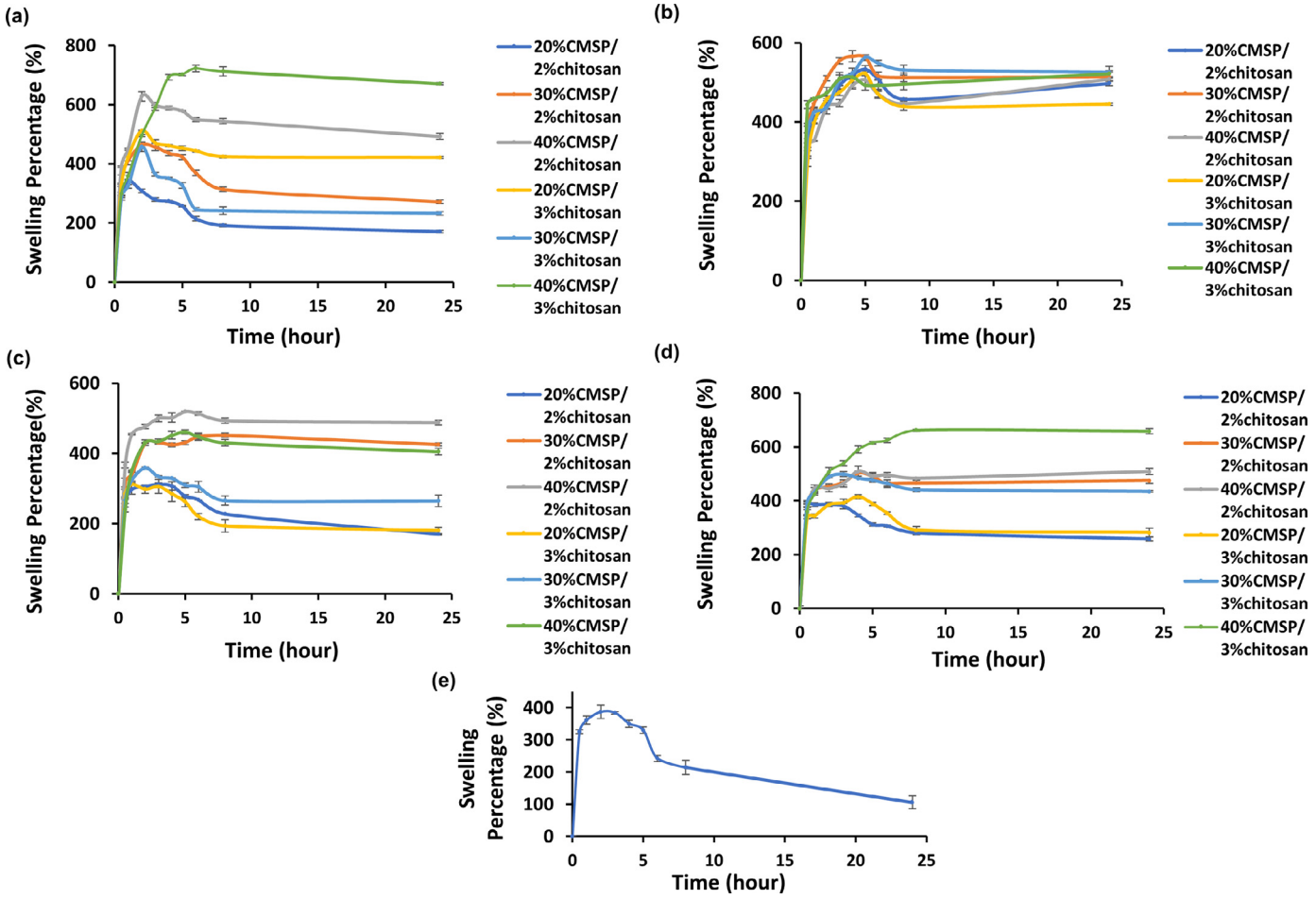

Fig. 3. Swelling percentage of various formulations of CMSP/ chitosan hydrogel discs in (a) distilled water, (b) pH 1.2, (c) pH 5.5 and (d) pH 7.4 buffer solution at room temperature (e) pH 7.4 buffer solution at 37°C of 40% CMSP/3% chitosan hydrogel.

Table 1
Drug loading and DEE in 40% CMSP/2% chitosan and 40% CMSP/3% chitosan hydrogel discs ($n = 3 \pm$ sd).

CMSP/Chitosan Hydrogel Disc loaded with Diclofenac Sodium	Weight of Hydrogel Discs (mg)	Drug Content of Hydrogel Discs (mg)	Drug Loading (%)	Theoretical Drug Content (mg)	Drug Encapsulation Efficiency (%)
40% CMSP/2% Chitosan	250.87 ± 8.91	41.94 ± 2.59	16.75 ± 1.57	75.26 ± 2.67	55.84 ± 5.24
40% CMSP/3% Chitosan	238.57 ± 3.19	46.78 ± 0.78	19.61 ± 0.07	71.57 ± 0.96	65.37 ± 0.24

Table 2
The diameter, thickness and weight of diclofenac sodium-loaded and unloaded 40% CMSP/3% chitosan hydrogel disc ($n = 3 \pm$ sd). Means within the same column with different alphabets are statistically different ($p < 0.05$).

CMSP/Chitosan Hydrogel Disc	Diameter (mm)	Thickness (mm)	Weight (mg)
40% CMSP/3% Chitosan (Unloaded)	5.84 ± 0.07	1.62 ± 0.07[a]	44.5 ± 2.3
40% CMSP/3% Chitosan (Drug-loaded)	5.89 ± 0.07	1.75± 0.11[b]	47.8 ± 2.2

loading of 40% CMSP/2% chitosan and 40% CMSP/3% chitosan was approximately 42% and 47%, respectively. Overall, CMSP/chitosan hydrogel discs have higher DEE than a previous study on calcium-crosslinked hydrogel beads, probably due to lesser drug loss during EB- induced cross-linking (Tan et al., 2016a). As 40% CMSP/3% chitosan hydrogel has higher drug loading and DEE, it was further tested in subsequent characterisation tests.

The hydrogel disc diameter was measured using a calliper (Fig. 4(A) a). The slight standard deviation of diameter, thickness, and weight for both unloaded and loaded 40% CMSP/3% chitosan hydrogel disc indicated that the discs are uniform (Table 2). In Table 2, the means within the same column with different alphabets are statistically different ($p < 0.05$). It was observed that the thickness of unloaded discs was significantly reduced as compared to the drug-loaded discs. This could be due to a higher degree of cross-linking in unloaded hydrogel and the hydrogel's shrinkage, resulting in thinner discs. Besides, for drug-loaded hydrogel discs, the polymer solution mixtures before irradiation cross-linking had higher viscosity and density. Therefore, there might be a reduction in the penetration of EB irradiation and a decrease in the cross-linking degree (Lam et al., 2015).

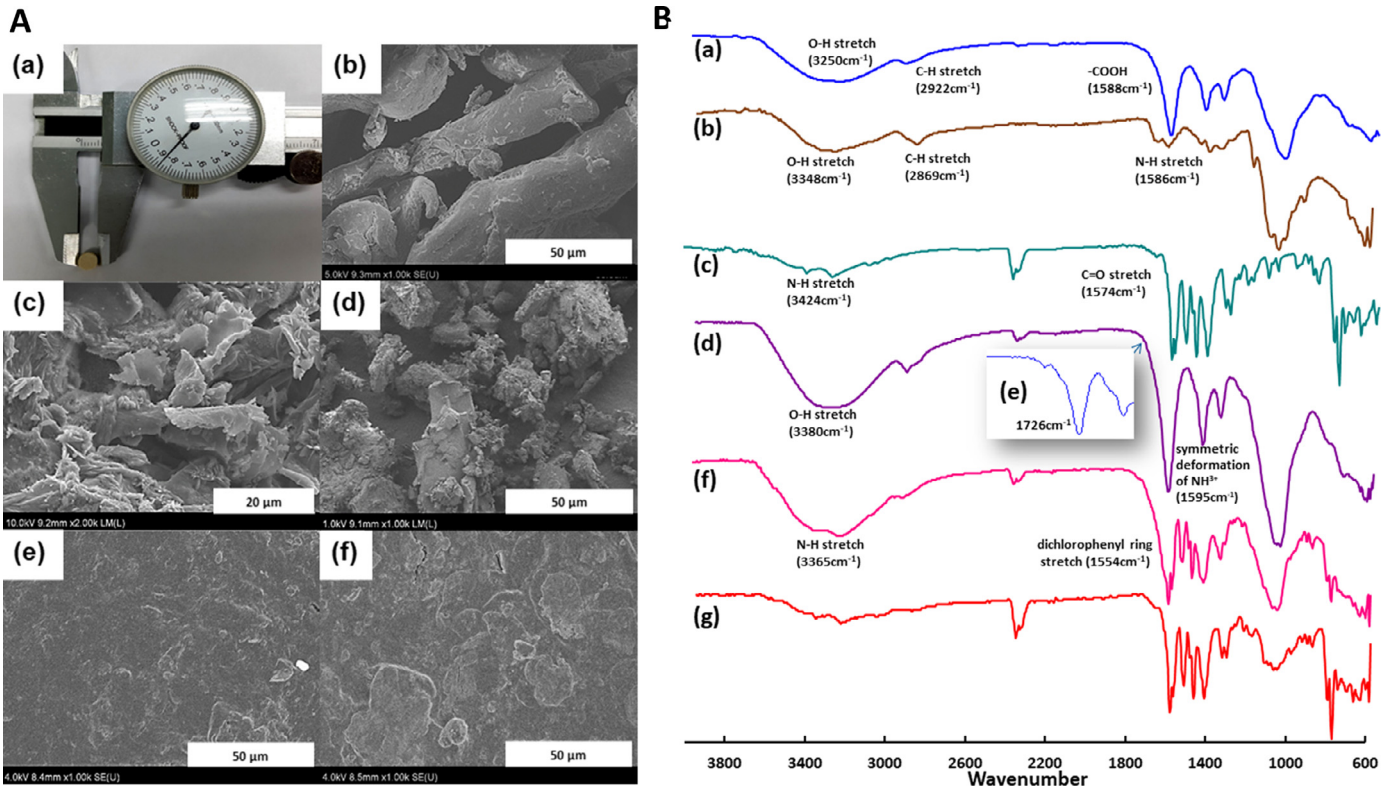

Fig. 4. (A) Measurement of hydrogel disc using a calliper (a), FESEM images of chitosan (b), CMSP (c), diclofenac sodium (d), unloaded 40% CMSP/3% chitosan hydrogel disc (e), and diclofenac sodium loaded 40% CMSP/3% chitosan (f). (B) FTIR spectra of CMSP (a), chitosan (b), diclofenac sodium (c), 40% CMSP/3% chitosan hydrogel (d), magnified formation of new peak in 40% CMSP/3% chitosan (e), and diclofenac sodium loaded 40% CMSP/3% chitosan (f), physical mixture of CMSP: chitosan: diclofenac sodium (g).

3.6. Field emission scanning electron microscopy (FESEM)

Based on the FESEM images, chitosan (Fig. 4A(b)) and CMSP (Fig. 4A(c)) had a smooth surface, whereas diclofenac sodium (Fig. 4A(d)) had a rough surface. The unloaded 40% CMSP/3% chitosan hydrogel disc had a smooth surface, indicating the extensive cross-linking between chitosan and CMSP had formed a compatible matrix (Fig. 4A(e)). However, diclofenac sodium-loaded 40% CMSP/ 3% chitosan hydrogel discs had rougher surfaces (Fig. 4A(f)). This could be attributed to the presence of the diclofenac sodium that caused a low polymer to drug ratio, prevented the penetration of EB radiation, and reduced the cross-linking of polymers. As shown in Fig. 4A(f), there were no visible drug particles on the surface of the drug-loaded disc, indicating the inclusion of diclofenac sodium within the hydrogel matrix (Lam et al., 2015).

3.7. Fourier transform infrared (FTIR) spectroscopy

FTIR was carried out to determine the polymer-polymer and polymer-drug interactions. IR spectrum of CMSP showed a broad peak around 3250 cm^{-1}, indicated the stretching vibration for hydroxyl group (-OH) (Fig. 4B(a)). The peak at 2922 cm^{-1} showed the C-H stretching vibration of the carboxymethyl group. The existence of a strong absorption band at 1588 cm^{-1} confirmed the presence of carboxylic (COO^-) functional group corresponding to CMC structure obtained from carboxymethylation of sago pulp. Absorption bands at 1413 cm^{-1} and 1322 cm^{-1} represented -CH_2 stretching. The broad absorption peak around 1015 cm^{-1} represented C-O stretching vibration for the ether linkage of the 1,4-β-D-glucoside group (>CH-O-CH<) of cellulose backbone (Biswal & Singh, 2004).

For chitosan (Fig. 4B(b)), there was a broad absorption band centred at 3348 cm^{-1} due to stretching vibration of O-H and overlapped with extension vibration of N-H as well as intermolecular H-bonds. The absorption spectrum at 2869 cm^{-1} showed axial stretching of C-H bonds. The peak at 1641 cm^{-1} showed carbonyl group of amide resulted from incomplete deacetylation of chitin to chitosan (amide I). The angular deformation of N-H bonds of the amino groups (amide II) was shown at 1586 cm^{-1} (L. Zhang, Wang, Guo, & Ma, 2014). The band at 1374 cm^{-1} indicated symmetrical angular deformation of CH_3, while 1149 cm^{-1} illustrated the asymmetric vibration of C-O in the oxygen bridge due to deacetylation of chitosan. The evidence of the presence of polysaccharides skeleton was shown in the absorption spectrum range from 1061 cm^{-1} to 893 cm^{-1}. This included C-O-C in a glycosidic linkage, C-H vibration indicated by absorption spectrum at 1061 cm^{-1}, and visible -CONH- group at 1025 cm^{-1} (Murtaza, Ahmad, & Shahnaz, 2010).

For diclofenac sodium (Fig. 4B(c)), the absorption spectrum at 3424 cm^{-1} indicated NH stretching of the secondary amine. The absorption peak observed at 1574 cm^{-1} represented the -C=O stretching of the carboxyl ion, and absorption peak at 769 cm^{-1} showed the C-Cl stretching. The absorption peak at 1552 cm^{-1} represented the dichlorophenyl ring. Other than that, C-O stretching was indicated by the absorption peak at 1309 cm^{-1} while C-CO-C stretching was shown by the absorption peak at 1289 cm^{-1}.

For unloaded 40% CMSP/3% chitosan hydrogel disc (Fig. 4B(d)), a new weak shoulder peak at 1726 cm^{-1} indicated the interaction between -COOH groups of CMSP and -NH_2 groups of chitosan in Fig. 4B(e). The presence of the band at 1595 cm^{-1} represented the symmetric deformation of NH_3^+ ion, owing to the electrostatic interaction of cationic groups from chitosan and anionic groups from CMSP to form an intermacromolecular complex (Grumezescu et al., 2012; Rosca, Popa, Lisa, & Chitanu, 2005).

For diclofenac sodium-loaded 40% CMSP/3% chitosan disc, the distinctive peak at 3365 cm^{-1} represented NH stretching of the sec-

ondary amine (Fig. 4B(f)). The characteristic peak at 760 cm^{-1} was due to C-Cl stretching and the absorption peak at 1554 cm^{-1} indicated dichlorophenyl ring in the diclofenac sodium structure. There was no appearance of new absorption band for drug-loaded hydrogel mixture as compared to the unloaded hydrogel, indicated the absence of chemical interaction between diclofenac sodium with CMSP and chitosan. Besides, the functional groups of the drug in drug-loaded hydrogel have not been altered. As evidenced by the same pattern of IR spectrum of physical mixture of CMSP, chitosan, and diclofenac sodium in 1:1:1 ratio shown in Fig. 4B (g), the presence of diclofenac sodium in CMSP/chitosan hydrogel disc has been verified.

3.8. Differential scanning calorimetry (DSC)

The thermal profile of CMSP exhibited endothermic melting peaks at 176 °C and 193 °C. Both endothermic peaks were associated with structural transitions of the polymer chains (Fig. 5A(a)) (Łojewska, Miśkowiec, Łojewski, & Proniewicz, 2005). Below 220 °C, the structural transition might be related to partial oxidation of OH groups on the polymer chains as the oxidation of OH groups was difficult due to the attachment to the sugar ring (Li, Sun, & Wu, 2009). The endothermic peaks at 300–330 °C for CMSP could be due to the decomposition of the CMSP chain (Lam et al., 2015).

The thermal profile of chitosan exhibited two endothermic peaks at 162 °C and 183 °C, which might be due to dissociation of interchain hydrogen bonding of chitosan formed at an amino group and hydroxyl functional group (Fig. 5A(b)) (El-Hefian, Elgannoudi, Mainal, & Yahaya, 2010). The exothermic peak at about 330 °C could be due to the thermal decomposition of chitosan (Kumar & Koh, 2012). In Fig. 5A(c), two endothermic peaks were observed from thermograms for 40% CMSP/3% chitosan hydrogel at 167 °C and 191 °C. This indicated the thermal property in between CMSP and chitosan as the peaks shifted to fall within the melting points of CMSP and chitosan.

As represented in Fig. 5A(d), the thermogram of diclofenac sodium exhibited a sharp endothermic peak at 301 °C, showing its melting point (Tudja, Khan, MEŠTROVIC, Horvat, & Golja, 2001). The peak at 164 °C indicated a complete loss of water molecules.

Based on the DSC thermogram of diclofenac sodium-loaded 40% CMSP/3% chitosan hydrogel disc (Fig. 5A(e), there was a presence of a new endothermic peak at 268 °C that corresponds to the incorporation of diclofenac sodium. This showed that diclofenac sodium has remained in the crystalline state in the polymer matrix. The detection of a lower melting point peak than the melting peak detected in the pure drug could be due to the polymorphic transition of the drug (Tudja et al., 2001). The broad exothermic peaks in unloaded and diclofenac sodium-loaded 40% CMSP/3% chitosan hydrogel disc indicated the degradation of polymer (Jelvehgari, Valizadeh, Jalali Motlagh, & Montazam, 2014).

3.9. Thermogravimetric analyses (TGA)

Another thermal analysis, TGA, was carried out to further characterise the thermal property of the fabricated hydrogel disc. The weight loss of about 11% at around 110 °C for CMSP hydrogel disc was due to loss of water moisture (Fig. 5B). Besides, there was a rapid weight loss at about 250–340 °C with a weight loss of 30%, indicated the loss of carbon dioxide from carboxymethyl groups of CMSP due to thermal degradation (Su, Huang, Yuan, Wang, & Li, 2010). Chitosan showed two stages of degradation. The initial degradation occurred at around 60 °C and displayed 10% weight loss due to the loss of water molecules. The second stage of degradation occurred at around 280–350 °C with a weight loss of 43% was assigned to the thermal and oxidative decomposition of chitosan, elimination of volatile products, and vaporisation (Neto et al., 2005; Tirkistani, 1998). Thermal decomposition of CMSP/chitosan dried hydrogel was investigated in several stages. The weight loss of 40% CMSP/3% chitosan hydrogel disc (9%) during heating at around 110°C indicated evaporation of water molecules. The weight-loss rates increased from 250–330 °C and displayed 31% weight loss. The result showed that the thermal stability of CMSP/chitosan hydrogel is similar to the thermal stability of CMSP due to its higher composition in this composite material.

3.10. X-ray diffraction (XRD)

Based on Fig. 5C(a) and (c), the presence of a broad peak for CMSP and chitosan indicated the amorphous state of CMSP and chitosan. The second broad peak of chitosan was absent in the CMSP/chitosan hydrogel mixture (Fig. 5C(b)). This might be due to the formation of an electrostatic interaction between an amino group from chitosan and carboxyl group from CMSP, weakened the intra- and intermolecular hydrogen bonds that caused crystallisation (Kaihara, Suzuki, & Fujimoto, 2011). Diclofenac sodium was in the crystalline state (Fig. 5C(d)), with peaks at about 6, 8, 15, 20, 25, 26 and 27° at 2θ values (Shivakumar, Desai, & Deshmukh, 2008). However, the absence of the peak in the unloaded 40% CMSP/3% chitosan hydrogel disc indicated the amorphous state of chitosan and CMSP in the hydrogel disc. The diffractogram of diclofenac sodium-loaded hydrogel showed the presence of crystalline diclofenac sodium in the disc (Fig. 5C(e)). This could be due to the existence of diclofenac sodium in microcrystalline form within the polymer matrix when the drug concentration has exceeded the solubility in the polymer matrix (Shivakumar et al., 2008). The diffractogram of the physical mixture of CMSP, chitosan and diclofenac sodium with a ratio of 1:1:1 showed the same pattern as diclofenac sodium-loaded 40% CMSP/3% chitosan hydrogel (Fig. 5C(f)), where the amorphous state of both chitosan and CMSP remained in the hydrogel disc.

3.11. In vitro drug release

For *in vitro* drug release study, pH 1.2 and pH 6.8 release media were used to simulate gastric fluid (pH 1.2) and intestinal fluid (pH 6.8), based on the guidelines in United States Pharmacopeia, for drug release study of diclofenac sodium (United States Pharmacopeia, 2004). Fig. 5D showed the cumulative release of diclofenac sodium from 40% CMSP/3% chitosan hydrogel disc against time at pH 1.2 for 2 h and continued at pH 6.8 at 37 °C, simulating the colonic environment. At the first 2 h, less than 5% of diclofenac sodium was released. At the 3rd hour, the release of diclofenac sodium became faster due to the release of loosely entrapped drug in the swollen hydrogel disc. A slow and sustained drug release was observed from 4 to 16 h. As time progressed, the drug release rate decreased and eventually reached a plateau at the 32^{nd} h. This could be explained by the increase in the path length for diclofenac sodium molecule to diffuse toward dissolution medium and the remaining drug was entrapped in the inner part of hydrogel matrix (Lam et al., 2015). In acidic medium, the COO^- group in CMSP and amino group in chitosan were protonated, created strong electrostatic forces. The hydrogel disc remained unswollen and restricted the release of diclofenac sodium. At pH 6.8, osmotic swelling forces built up due to deprotonation of COO^- group of CMSP and amino group of chitosan. Thus, there was a faster release of diclofenac sodium. The high solubility of diclofenac sodium above its pK_a value contributed to the faster release of the drug into the buffer solution (Lina Zhang et al., 2001). Besides, it was observed that the discs swelled steadily and increased in size as time progressed. However, after 15 h, the hydrogel has started to degrade and no longer staying intact. The reading slightly fluctuated after 20 h. The results showed that the diclofenac sodium-loaded 40% CMSP/3% chitosan hydrogel disc could exhibit the pH-sensitive and sustained release up to 32 h. Based on the study conducted by Jose et al., formulations with the high initial release of drug was not ideal for colonic drug delivery as the drug was supposed to be released in the colon (Jose, Dhanya, Cinu, & Aleykutty, 2010). Thus, the drug release system in this study is potential for continuous release of medication with therapeutic effect over an extended period in the colon after the administration of a single dose.

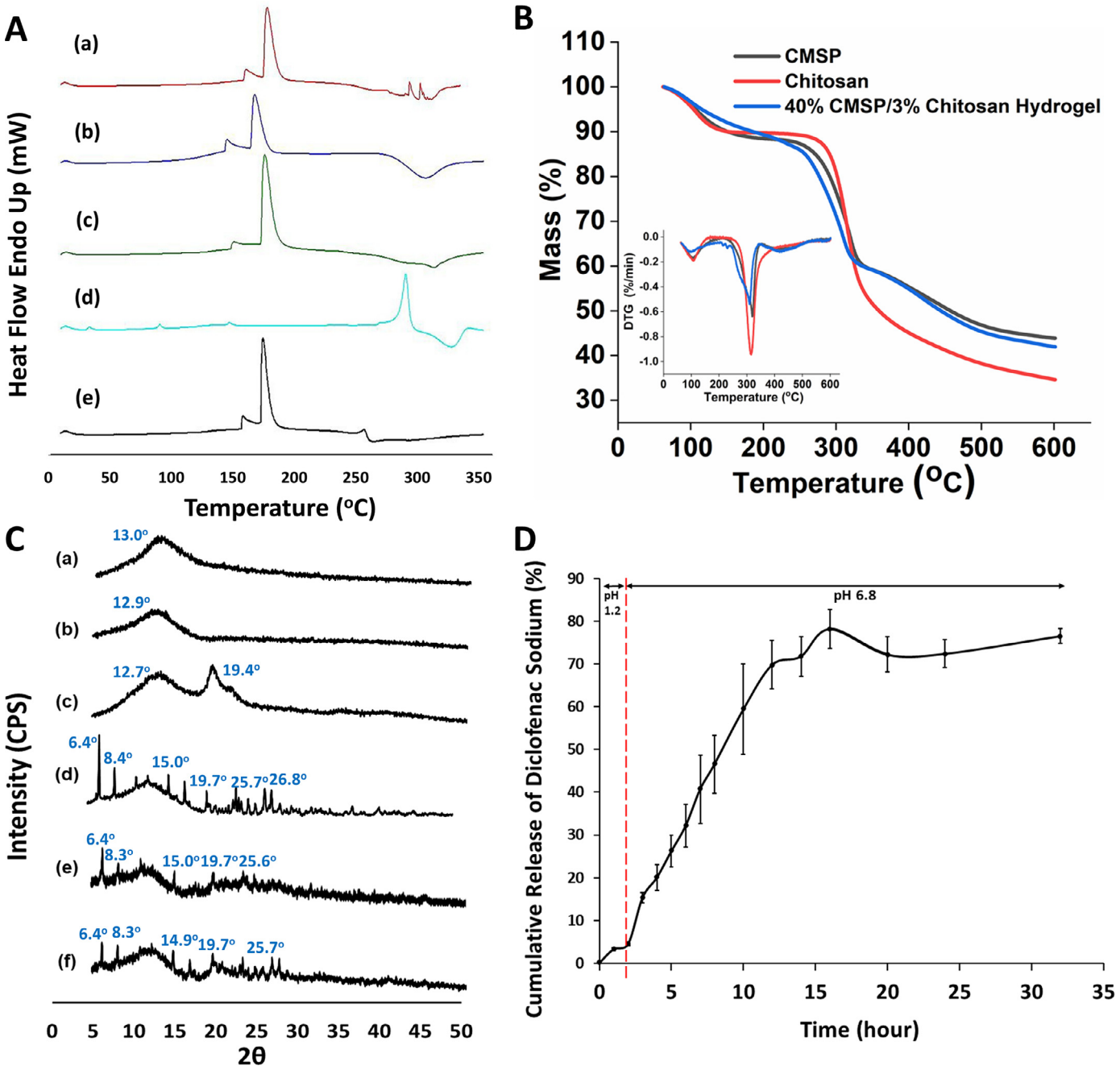

Fig. 5. (A) DSC thermograms of CMSP (a), chitosan (b), unloaded 40% CMSP/3% chitosan (c), diclofenac sodium (d), and loaded 40% CMSP/3% chitosan hydrogel disc (e). (B) TGA and DTG curves of CMSP (a), chitosan (b), and unloaded 40% CMSP/3% chitosan hydrogel disc (c). (C). X-ray diffraction of CMSP (a), unloaded 40% CMSP/3% chitosan (b), chitosan (c), diclofenac sodium (d), drug-loaded 40% CMSP/3% chitosan (e) disc and physical mixture of diclofenac sodium, CMSP and chitosan (f). (D) The graph of cumulative release of diclofenac sodium from 40% CMSP/3% chitosan hydrogel disc against time.

3.12. Drug release kinetics

The data of *in vitro* release was further analysed through the mechanism and mathematical modelling to investigate the drug release from hydrogel (Saravanan, Bhaskar, Maharajan, & Pillai, 2004).

Table 3 showed the best fit with a higher correlation coefficient (r^2=0.9910) was shown in first order model if compared to (r^2= 0.9683) for the zero-order model. This could be attributed to the tightly bound diclofenac sodium in the polymer matrix, which caused the release of diclofenac sodium to be directly proportional to the amount of diclofenac sodium remained in the polymer matrix with the slow sustained release. It was believed that three steps have occurred for drug release. This included inhibition of surrounding medium into hydrogels, dissolution of the drug from hydrogel, and diffusion release of the drug into the surrounding medium Peppas (1985).

A graph of cumulative percentage of drug release versus square root of time was plotted for Higuchi model (Eq. 8):

$$Qt = kH(t)\ 0.5 \tag{8}$$

where k_H is the release constant. The correlation coefficient (r^2=0.793) was obtained, which indicated the release of diclofenac sodium from CMSP/chitosan hydrogel disc was not diffusion-controlled. Therefore, to verify the mechanism of drug release, the Korsmeyer-Peppas model

Table 3
The coefficient, *in vitro* release rate and the rate exponent of diclofenac sodium from 40% CMSP/ 3% chitosan hydrogel disc.

	Zero order		First order		Higuchi		Korsmeyer-Peppas	
	Correlation coefficient (r^2)	Rate constant, k_o (h^{-1})	Correlation coefficient (r^2)	Rate constant, k_1 (h^{-1})	Correlation coefficient (r^2)	Higuchi dissolution constant, k_H ($h^{-1/2}$)	Correlation coefficient (r^2)	*n* value
Diclofenac sodium	0.9683	5.3431	0.9910	0.1011	0.7930	17.100	0.9970	1.157

*r^2 is the correlation coefficient and release rate constants k_0, k_1 and k_H was calculated from the slope of the plot, respectively.

Table 4
Measurements of the diameter of the zone of inhibitions in disk-diffusion test.

Test microorganisms	Zone of Inhibitions (Diameter/mm)			
	CMSP 20%/ chitosan 2%, (unloaded)	CMSP 30%/ chitosan 2%, (unloaded)	CMSP 40%/ chitosan 2%, (loaded with 16.75% of diclofenac sodium)	CMSP 40%/ chitosan 3%, (loaded with 19.61% of diclofenac sodium)
Methicillin resistant *Staphylococcus aureus* (MRSA)	10.7	9.4	14.2	13.6
Enterococcus faecalis	8.7	9.6	9.1	8.4
Klebsiella pneumoniae	5.8	6.2	16.6	15.5
Proteus mirabilis	7.7	10.2	13.9	12.8
Escherichia coli	9.3	10.1	8.6	11.9
Pseudomonas aeruginosa	9.8	9.4	8.9	9.1

was used (Eq. 9):

$$Mt/Ma = Ktn \quad (9)$$

where M_t/M_a is the proportion of drug released at time *t*, *k* is rate constant, and *n* is the exponent value Peppas (1985).

The release of the diclofenac sodium hydrogel disc in pH 6.8 was a super case II transport with a correlation coefficient (r^2=0.9970) and n value of 1.157 (Table 3). Hence, the release kinetics studies clearly stated that the drug released was a combination of swelled-controlled, diffusion, relaxation, and the erosion of polymer matrix (Hosseinzadeh, 2010).

3.13. Antimicrobial activity of CMSP/chitosan hydrogel discs

Antimicrobial study was carried on unloaded CMSP 20%/chitosan 2%, unloaded CMSP 30%/chitosan 2%, diclofenac sodium loaded CMSP 40%/ chitosan 2%, and diclofenac sodium loaded CMSP 40%/chitosan 3% hydrogels, using disk diffusion method. Pure diclofenac sodium exists in powder form, which was in a different form from the hydrogel discs. Considering the possible difference in drug release rates and antimicrobial effect, pure diclofenac sodium powder was not included in this experiment. All types of hydrogel discs showed the formation of an inhibition zone of the growth of the bacteria. The zone of inhibition diameters varied between 5.8 to 16.6 mm (Table 4).

Considering the diameter of the zone of inhibitions as shown Fig. 6, it was observed that the zone of inhibitions of the discs loaded with diclofenac sodium was larger than the unloaded discs. It was previously reported that both chitosan and diclofenac sodium effectively suppress the growth of pathogenic bacterial strains (Annadurai, Basu, Ray, Dastidar, & Chakrabarty, 1998; Kaya, Asan-Ozusaglam, & Erdogan, 2016). The antimicrobial efficacy of chitosan depends on but is not limited to (1) positive charge density. Previous literature have shown the importance of polycationic structures, which have a profound effect on the antibacterial activity, due to the higher electrostatic interactions between the side chains and the outer membrane of the bacteria (Kong et al., 2008; Takahashi, Imai, Suzuki, & Sawai, 2008), (2) molecular weight of chitosan (Mw): several studies previously performed on the antibacterial activity of chitosan with respect to the Mw were found to be ambiguous. Some studies on *E. coli* have reported that the chitosan with high Mw showed higher antimicrobial activity than the low Mw chitosan. In addition, the same activity was shown against *E.coli* and *B. subtillis* irrespective of the Mw (Tikhonov et al., 2006). Antimicrobial activity was also reported for low Mw chitosan by few researchers (Tokura, Ueno, Miyazaki, & Nishi, 1996), (3) hydrophilic/hydrophobic characteristic and chelating capacity: irrespective of the different parameters that contribute to the antibacterial activity of chitosan, water plays a critical role and as the completely dry samples are incapable of interacting with the microorganisms. Hence depending on the hydrophobicity/hydrophilicity, the antimicrobial activity of chitosan varies. Chitosan has been found to possess the high chelating ability for various metal ions that combine with cell wall molecules of microorganism Kurita (1998). These metal ions play a crucial role in the stability of the cell wall, and this chelation activity has often been suspected as one of the possible modes of antimicrobial action (Rabea, Badawy, Stevens, Smagghe, & Steurbaut, 2003). Chitosan is effective against both gram +ve and gram –ve bacteria, which mainly attributed to its interaction with the negatively charged lipoproteins (LPS) and the peptidoglycan layer which are the outer layers present in the gram -ve and gram +ve bacteria respectively (Silhavy, Kahne, & Walker, 2010). It participates in a series of elementary processes leading to the biocidal activity which include (1) adsorption onto the bacterial cell surface which involves the simple surface binding due to the attraction of opposite charges (2) diffusion through the outer membrane allowing the polymer to penetrate into the bilayer, causing expansion, thereby decreasing the phase transition temperature and altering the permeability of the cell outer membrane, which in turn leads to the adsorption onto the cytoplasmic membrane. Disruption of the cytoplasmic membrane occurs following the adsorption of the polymer leading to the leakage of the cytoplasmic constituents, and death of the bacteria (Chen & Cooper, 2002; Ikeda, Tazuke, & Suzuki, 1984). Based on the results in this study, the antibacterial effects of chitosan and diclofenac sodium was observed. Therefore, other than serving as the hydrogel with intrinsic antimicrobial activity, the hydrogel could also serve as a potential alternative drug carrier for antimicrobial treatment, to tackle the global challenge of antimicrobial resistance.

4. Conclusion

CMSP from sago waste with a degree of substitution 0.8 has been cross-linked with chitosan by EB irradiation to form a hydrogel that carries diclofenac sodium. CMSP/chitosan hydrogel exhibited pH-sensitive and temperature-sensitive behaviour. FTIR results showed that di-

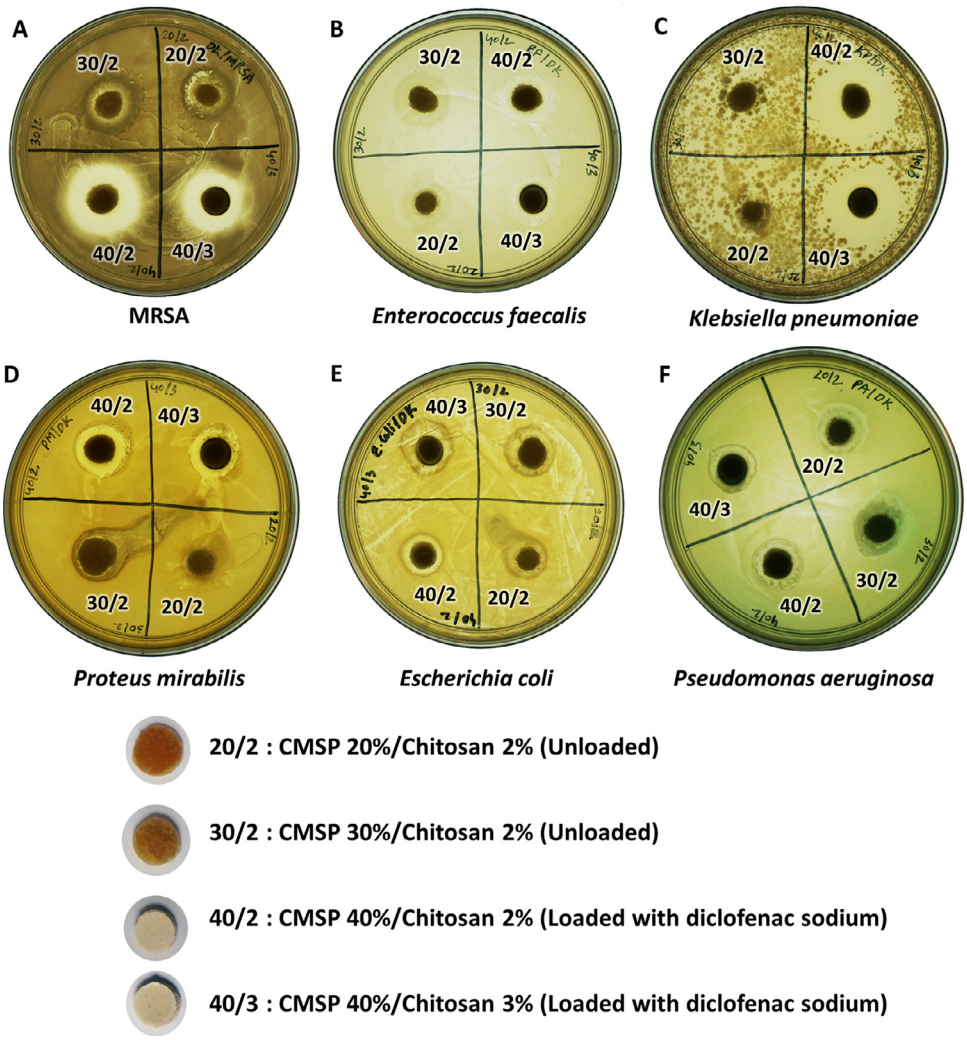

Fig. 6. Antimicrobial activity of CMSP 20%/chitosan 2% (unloaded), CMSP 30%/chitosan 2% (unloaded), CMSP 40%/chitosan 2% (loaded with 16.75% of diclofenac sodium) and CMSP 40%/chitosan 3% (loaded with 19.61% of diclofenac sodium) against MRSA, *Enterococcus faecalis, Klebsiella pneumoniae, Proteus mirabilis, Escherichia coli, Pseudomonas aeruginosa.*

clofenac sodium remained stable and did not undergo any chemical changes after EB irradiation. XRD and DSC analysis revealed the amorphous state of CMSP and chitosan and crystalline state of diclofenac sodium. TGA results showed no change in the thermal behaviour of 40% CMSP/3% chitosan hydrogel. A low amount of diclofenac sodium (< 5%) was released at stomach pH (pH 1.2), and showing slow, sustained release with kinetics obeying first-order's model in the colonic pH (pH 6.8) with sustained-release up to 32 h. This hydrogel has also exhibited antimicrobial activity. All results showed that 40% CMSP/3% chitosan hydrogel disc would be a potential drug carrier for colon-targeted delivery that will improve the bioavailability in the colon and reduce the frequency of administration.

Conflicts of Interest

The authors declare no conflicts of interest in this work.

Acknowledgements

This study was funded by the School of Science of Monash University Malaysia. The authors would like to acknowledge Malaysia Nuclear Agency for EB irradiation facility.

References

Almáši, M., Beňová, E., Zeleňák, V., Madaj, B., Huntošová, V., Brus, J., & Hornebecq, V. (2020). Cytotoxicity study and influence of SBA-15 surface polarity and pH on adsorption and release properties of anticancer agent pemetrexed. *Materials Science and Engineering C, 109*, Article 110552.

Alves, N. M., & Mano, J. F. (2008). Chitosan derivatives obtained by chemical modifications for biomedical and environmental applications. *International Journal of Biological Macromolecules, 43*(5), 401–414.

Annadurai, S., Basu, S., Ray, S., Dastidar, S., & Chakrabarty, A. (1998). Antibacterial activity of the antiinflammatory agent diclofenac sodium. *Indian journal of experimental biology, 36*(1), 86–90.

Bashir, S., Teo, Y. Y., Naeem, S., Ramesh, S., & Ramesh, K. (2017). pH responsive N–succinyl chitosan/Poly (acrylamide-co-acrylic acid) hydrogels and in vitro release of 5-fluorouracil. *PLOS ONE, 12*(7), Article e0179250.

Biswal, D. R., & Singh, R. P. (2004). Characterisation of carboxymethyl cellulose and polyacrylamide graft copolymer. *Carbohydrate Polymers, 57*(4), 379–387.

Bucci, R., Magrì, A. D., & Magrì, A. L. (1998). Determination of diclofenac salts in pharmaceutical formulations. *Fresenius Journal of Analytical Chemistry, 362*(7), 577–582.

Chang, C., & Zhang, L. (2011). Cellulose-based hydrogels: Present status and application prospects. *Carbohydrate Polymers, 84*(1), 40–53.

Chen, C. Z., & Cooper, S. L. (2002). Interactions between dendrimer biocides and bacterial membranes. *Biomaterials, 23*(16), 3359–3368.

El-Hefian, E. A., Elgannoudi, E. S., Mainal, A., & Yahaya, A. H. B (2010). Characterization of chitosan in acetic acid: Rheological and thermal studies. *Turkish Journal of Chemistry, 34*(1), 47–56.

Fan, D.-y., Tian, Y., & Liu, Z.-j. (2019). Injectable hydrogels for localized cancer therapy. *Frontiers in Chemistry, 7*(675).

Fei, B., Wach, R. A., Mitomo, H., Yoshii, F., & Kume, T. (2000). Hydrogel of biodegradable cellulose derivatives. I. Radiation-induced crosslinking of CMC. *Journal of Applied Polymer Science, 78*(2), 278–283.

Gibaldi, M., & Feldman, S. (1967). Establishment of sink conditions in dissolution rate determinations. Theoretical considerations and application to nondisintegrating dosage forms. *Journal of Pharmaceutical Science, 56*(10), 1238–1242.

Grumezescu, A. M., Andronescu, E., Ficai, A., Bleotu, C., Mihaiescu, D. E., & Chifiriuc, M. C. (2012). Synthesis, characterization and in vitro assessment of the magnetic chitosan–carboxymethylcellulose biocomposite interactions with the prokaryotic and eukaryotic cells. *Journal of Pharmaceutical Science, 436*(1), 771–777.

Hosseinzadeh, H. (2010). Controlled release of diclofenac sodium from pH-responsive carrageenan-g-poly(acrylic acid) superabsorbent hydrogel. *Journal of Chemical Sciences, 122*(4), 651–659.
Ikeda, T., Tazuke, S., & Suzuki, Y. (1984). Biologically active polycations, 4. Synthesis and antimicrobial activity of poly(trialkylvinylbenzylammonium chloride)s. *Die Makromolekulare Chemie, 185*(5), 869–876.
Jelvehgari, M., Valizadeh, H., Jalali Motlagh, R., & Montazam, H. (2014). Formulation and physicochemical characterization of buccoadhesive microspheres containing diclofenac sodium. *Advanced Pharmaceutical Bulletin, 4*(3), 295–301.
Jose, S., Dhanya, K., Cinu, T., & Aleykutty, N. (2010). Multiparticulate system for colon targeted delivery of ondansetron. *Indian J Pharm Sci, 72*(1), 58.
Kaihara, S., Suzuki, Y., & Fujimoto, K. (2011). In situ synthesis of polysaccharide nanoparticles via polyion complex of carboxymethyl cellulose and chitosan. *Colloids and Surfaces B: Biointerfaces, 85*(2), 343–348.
Kaya, M., Asan-Ozusaglam, M., & Erdogan, S. (2016). Comparison of antimicrobial activities of newly obtained low molecular weight scorpion chitosan and medium molecular weight commercial chitosan. *Journal of Bioscience and Bioengineering, 121*(6), 678–684.
Khan, M. A. (2012). Studies of the effect of pH oer dissolution profile of diclofenac sodium sustained release tablets. *Journal of Drug Delivery and Therapeutics, 2*(5).
Kong, M., Chen, X.-g., Xue, Y.-p., Liu, C.-s., Yu, L.-j., Ji, Q.-x., & Park, H. J. (2008). Preparation and antibacterial activity of chitosan microshperes in a solid dispersing system. *Frontiers of Materials Science, 2*(2), 214–220.
Kumar, S., & Koh, J. (2012). Physiochemical, optical and biological activity of chitosan-chromone derivative for biomedical applications. *International Journal of Molecular Sciences, 13*(5), 6102–6116.
Kurita, K. (1998). Chemistry and application of chitin and chitosan. *Polymer Degradation and Stability, 59*(1), 117–120.
Lam, Y. L., Muniyandy, S., Kamaruddin, H., Mansor, A., & Janarthanan, P. (2015). Radiation cross-linked carboxymethyl sago pulp hydrogels loaded with ciprofloxacin: Influence of irradiation on gel fraction, entrapped drug and in vitro release. *Radiation Physics and Chemistry, 106*(Supplement C), 213–222.
Li, W., Sun, B., & Wu, P. (2009). Study on hydrogen bonds of carboxymethyl cellulose sodium film with two-dimensional correlation infrared spectroscopy. *Carbohydrate Polymers, 78*(3), 454–461.
Łojewska, J., Miśkowiec, P., Łojewski, T., & Proniewicz, L. M. (2005). Cellulose oxidative and hydrolytic degradation: In situ FTIR approach. *Polymer Degradation and Stability, 88*(3), 512–520.
Long, D. D., & Luyen, D. V. (1996). Chitosan-carboxymethylcellulose hydrogels as supports for cell immobilization. *Journal of Macromolecular Science, Part A, 33*(12), 1875–1884.
Martinez-Ruvalcaba, A., Sánchez-Díaz, J., Becerra, F., Cruz-Barba, L., & González-Álvarez, A. (2009). Swelling characterization and drug delivery kinetics of polyacrylamide-co-itaconic acid/chitosan hydrogels. *eXPRESS Polymer Letters, 3*(1), 25–32.
Mulye, N. V., & Turco, S. J. (1995). A simple model based on first order kinetics to explain release of highly water soluble drugs from porous dicalcium phosphate dihydrate matrices. *Drug Development and Industrial Pharmacy, 21*(8), 943–953.
Murtaza, G., Ahmad, M., & Shahnaz, G. (2010). Microencapsulation of diclofenac sodium by nonsolvent addition technique. *Tropical Journal of Pharmaceutical Research, 9*(2).
Nargave, G. K., Singh, N., & Kondalkar, A. (2016). Development of colon targeted drug delivery system of diclofenac sodium using xylan as carrier. *Inventi Rapid: Pharm Tech, 4*, 1–13.
Neto, C. G. T., Giacometti, J. A., Job, A. E., Ferreira, F. C., Fonseca, J. L. C., & Pereira, M. R (2005). Thermal analysis of chitosan based networks. *Carbohydrate Polymers, 62*(2), 97–103.
Nisar, S., Pandit, A. H., Wang, L.-F., & Rattan, S. (2020). Strategy to design a smart photocleavable and pH sensitive chitosan based hydrogel through a novel crosslinker: a potential vehicle for controlled drug delivery. *RSC Advances, 10*(25), 14694–14704.
O'Neill, T. J., Nguemo, J. D., Tynan, A.-M., Burchell, A. N., & Antoniou, T. (2017). Risk of colorectal cancer and associated mortality in HIV: A systematic review and meta–analysis. *Journal of Acquired Immune Deficiency Syndromes, 75*(4), 439–447.
Pandey, M., Mohd Amin, M. C. I., Ahmad, N., & Abeer, M. M (2013). Rapid synthesis of superabsorbent smart-swelling bacterial cellulose/acrylamide-based hydrogels for drug delivery. *International Journal of Polymer Science, 2013*, Article 905471.
Peppas, N. A. (1985). Analysis of Fickian and non-Fickian drug release from polymers. *Pharm Acta Helv, 60*(4), 110–111.
Pourjavadi, A., Jahromi, P. E., Seidi, F., & Salimi, H. (2010). Synthesis and swelling behavior of acrylatedstarch-g-poly (acrylic acid) and acrylatedstarch-g-poly (acrylamide) hydrogels. *Carbohydrate Polymers, 79*(4), 933–940.
Prado da Silva, M. H., Moura, F. N., Navarro da Rocha, D., Gobbo, L. A., Costa, A. M., & Louro, L. H. L (2014). Zinc-modified hydroxyapatite coatings obtained from parascholzite alkali conversion. *Surface and Coatings Technology, 249*, 109–117.
Pushpamalar, V., Langford, S. J., Ahmad, M., Hashim, K., & Lim, Y. Y. (2013). Preparation of carboxymethyl sago pulp hydrogel from sago waste by electron beam irradiation and swelling behavior in water and various pH media. *Journal of Applied Polymer Science, 128*(1), 451–459.
Pushpamalar, V., Langford, S. J., Ahmad, M., & Lim, Y. Y. (2006). Optimization of reaction conditions for preparing carboxymethyl cellulose from sago waste. *Carbohydrate Polymers, 64*(2), 312–318.
Qiu, Y., & Park, K. (2001). Environment-sensitive hydrogels for drug delivery. *Advanced Drug Delivery Reviews, 53*(3), 321–339.
Rabea, E. I., Badawy, M. E. T., Stevens, C. V., Smagghe, G., & Steurbaut, W (2003). Chitosan as antimicrobial agent: applications and mode of action. *Biomacromolecules, 4*(6), 1457–1465.
Rajpurohit, H., Sharma, P., Sharma, S., & Bhandari, A. (2010). Polymers for colon targeted drug delivery. *Indian J Pharm Sci, 72*(6), 689–696.
Reddy, K. O., Uma Maheswari, C., Muzenda, E., Shukla, M., & Rajulu, A. V. (2016). Extraction and characterization of cellulose from pretreated ficus (peepal tree) leaf fibers. *Journal of Natural Fibers, 13*(1), 54–64.
Rosca, C., Popa, M. I., Lisa, G., & Chitanu, G. C. (2005). Interaction of chitosan with natural or synthetic anionic polyelectrolytes. 1. The chitosan–carboxymethylcellulose complex. *Carbohydrate Polymers, 62*(1), 35–41.
Sampath, U., Gunathilake, T. M., Ching, Y. C., Chuah, C. H., Rahman, N. A., & Nai-Shang, L. (2020). pH-responsive poly(lactic acid)/sodium carboxymethyl cellulose film for enhanced delivery of curcumin in vitro. *Journal of Drug Delivery Science and Technology, 58*, Article 101787.
Sangsuriyonk, K., Paradee, N., & Sirivat, A. (2020). Electrically controlled release of anticancer drug 5-fluorouracil from carboxymethyl cellulose hydrogels. *International Journal of Biological Macromolecules, 165*, 865–873.
Saravanan, M., Bhaskar, K., Maharajan, G., & Pillai, K. S. (2004). Ultrasonically controlled release and targeted delivery of diclofenac sodium via gelatin magnetic microspheres. *International Journal of Pharmacy, 283*(1-2), 71–82.
Seong, J. S., Yun, M. E., & Park, S. N. (2018). Surfactant-stable and pH-sensitive liposomes coated with N-succinyl-chitosan and chitooligosaccharide for delivery of quercetin. *Carbohydrate Polymers, 181*, 659–667.
Shivakumar, H. N., Desai, B. G., & Deshmukh, G. (2008). Design and optimization of diclofenac sodium controlled release solid dispersions by response surface methodology. *Indian Journal of Pharmaceutical Science, 70*(1), 22–30.
Silhavy, T. J., Kahne, D., & Walker, S. (2010). The bacterial cell envelope. *Cold Spring Harbor Perspectives in Biology, 2*(5), Article a000414.
Su, J.-F., Huang, Z., Yuan, X.-Y., Wang, X.-Y., & Li, M. (2010). Structure and properties of carboxymethyl cellulose/soy protein isolate blend edible films crosslinked by Maillard reactions. *Carbohydrate Polymers, 79*(1), 145–153.
Tahtat, D., Mahlous, M., Benamer, S., Nacer Khodja, A., Larbi Youcef, S., Hadjarab, N., & Mezaache, W. (2011). Influence of some factors affecting antibacterial activity of PVA/Chitosan based hydrogels synthesized by gamma irradiation. *Journal of Materials Science: Materials in Medicine, 22*(11), 2505–2512.
Takahashi, T., Imai, M., Suzuki, I., & Sawai, J. (2008). Growth inhibitory effect on bacteria of chitosan membranes regulated with deacetylation degree. *Biochemical Engineering Journal, 40*(3), 485–491.
Tan, H. L., Tan, L. S., Wong, Y. Y., Muniyandy, S., Hashim, K., & Pushpamalar, J. (2016a). Dual crosslinked carboxymethyl sago pulp/pectin hydrogel beads as potential carrier for colon-targeted drug delivery. *Journal of Applied Polymer Science, 133*(19).
Tan, H. L., Wong, Y. Y., Muniyandy, S., Hashim, K., & Pushpamalar, J. (2016b). Carboxymethyl sago pulp/carboxymethyl sago starch hydrogel: Effect of polymer mixing ratio and study of controlled drug release. *Journal of Applied Polymer Science, 133*(28).
Thenapakiam, S., Kumar, D. G., Pushpamalar, J., & Saravanan, M. (2013). Aluminium and radiation cross-linked carboxymethyl sago pulp beads for colon targeted delivery. *Carbohydrate Polymers, 94*(1), 356–363.
Tikhonov, V. E., Stepnova, E. A., Babak, V. G., Yamskov, I. A., Palma-Guerrero, J., Jansson, H.-B., & Varlamov, V. P. (2006). Bactericidal and antifungal activities of a low molecular weight chitosan and its N-/2(3)-(dodec-2-enyl)succinoyl/-derivatives. *Carbohydrate Polymers, 64*(1), 66–72.
Tirkistani, F. A. A (1998). Thermal analysis of some chitosan Schiff bases. *Polymer Degradation and Stability, 60*(1), 67–70.
Tokura, S., Ueno, K., Miyazaki, S., & Nishi, N. (1996). *Molecular Weight Dependent Antimicrobial Activity by Chitosan*. In M. Kamachi & A. Nakamura (Eds.), *New Macromolecular Architecture and Functions: Proceedings of the OUMS'95 Toyonaka, Osaka, Japan, 2–5 June, 1995* (pp. 199-207). Berlin, Heidelberg: Springer Berlin Heidelberg
Tudja, P., Khan, M. Z. I., MEŠTROVIC, E., Horvat, M., & Golja, P (2001). Thermal behaviour of diclofenac sodium: decomposition and melting characteristics. *Chemical and pharmaceutical bulletin, 49*(10), 1245–1250.
Ulański, P., Janik, I., & Rosiak, J. M. (1998). Radiation formation of polymeric nanogels. *Radiation Physics and Chemistry, 52*(1), 289–294.
Wen, P., Zhu, D.-H., Wu, H., Zong, M.-H., Jing, Y.-R., & Han, S.-Y. (2016). Encapsulation of cinnamon essential oil in electrospun nanofibrous film for active food packaging. *Food Control, 59*(Supplement C), 366–376.
Yoshii, F., Zhao, L., Wach, R. A., Nagasawa, N., Mitomo, H., & Kume, T. (2003). Hydrogels of polysaccharide derivatives crosslinked with irradiation at paste-like condition. *Nuclear Instruments and Methods in Physics Research Section B: Beam Interactions with Materials and Atoms, 208*(Supplement C), 320–324.
Zhang, L., Jin, Y., Liu, H., & Du, Y. (2001). Structure and control release of chitosan/carboxymethyl cellulose microcapsules. *Journal of Applied Polymer Science, 82*(3), 584–592.
Zhang, L., Wang, L., Guo, B., & Ma, P. X. (2014). Cytocompatible injectable carboxymethyl chitosan/N-isopropylacrylamide hydrogels for localized drug delivery. *Carbohydrate Polymers, 103*, 110–118.
Zhao, L., & Mitomo, H. (2008). Adsorption of heavy metal ions from aqueous solution onto chitosan entrapped CM-cellulose hydrogels synthesized by irradiation. *Journal of Applied Polymer Science, 110*(3), 1388–1395.